*Pure & Appl. Chem.*, Vol. 70, No. 6, pp. 1209–1215, 1998.
Printed in Great Britain.


# Modelling droplet impact in plasma spray processes

J. Mostaghimi

## ABSTRACT

A model is described to predict the splat shape in plasma spray process. The results show that the impact process is comprised of spreading and recoil. The degree of spreading increases with $Re^{.25}$; while spreading time is proportional to the ratio of the initial diameter to the impact speed. Under most conditions, simultaneous solidification plays a secondary role in arresting the spreading. Extension of the model to 3-dimensional situations and some preliminary results are also discussed.

## INTRODUCTION

Plasma spray coating is concerned with the deposition of powdered material onto substrates to form functional coatings. Powders fed into the plasma are heated, melted, and accelerated towards a substrate by the high temperature plasma to form dense coatings.

The produced coating is ultimately an agglomeration of individual droplets impacting over the substrate. Properties of the coating is largely determined by the thermodynamic state and velocity of the impacting particles, as well as the type of surface material and its preparation. The effect of the different plasma or other heat sources on the microstructure of the coatings is important because it determines the speed of the impacting particle as well as their thermodynamics state. Several investigators [1-3] have shown the sensitivity of the coatings microstructure to the shape and cooling rate of the splats.

Over the last 15 years, theoretical research in plasma spraying has been mainly focused on the particle heat and momentum transfer within the plasma. The heat transfer models, e.g., [4], predict the particle state up to the point of impact onto the substrate. They are not, however, designed to predict the dynamics of droplet impact and the splat shape.

### Previous Work on Droplet Impact

When a molten droplet impacts onto a cold substrate, it spreads and simultaneously solidifies. Several simple analytical models have been developed by a number of researchers [4-9]. These models predict the maximum spread of a droplet as a function of its impact conditions. Madjeski's approach, which is perhaps the most cited one, accounts for viscous energy dissipation, surface tension effects and simultaneous freezing of the splat. These models provide an estimate of the maximum degree of spread, but they fail to provide any information on recoil or dynamics of the spreading.

Development of a comprehensive model of droplet impact onto a surface of arbitrary shape requires the numerical solution of the 3-dimensional (3D) Navier-Stokes equations along with the energy equation. We note that a particular feature of this problem is that the shape of the impacting droplet with time must also be predicted.

The majority of numerical models have so far been concerned with the normal impact of a droplet onto a flat surface [10-17]. Under this condition, the problem becomes 2D and axisymmetric. Recently, Bussmann et. al. extended their model to 3D, which allows consideration of droplet impact onto surfaces of arbitrary geometry [18,19].

In this paper we describe a model that has been developed over the past five years at the University of Toronto's *Plasma Processing Laboratory* and discuss some of the important parameters affecting spreading and solidification of an impacting droplet.

## MATHEMATICAL MODEL

For the normal impact of a completely molten droplet we assume: a) the flow and heat transfer are 2D, axisymmetric, incompressible and laminar; b) heat transfer from the free surface is negligible compared with the heat transfer to the substrate; and c) negligible shear at the free surface.

In problems involving free surface flows, we need to predict the deformation of the surface versus time. This would be achieved by using the VOF (volume-of-fluid) method [20, 21]; where the Eulerian computational domain is divided into a number of cells and the governing partial equations are approximated by finite-difference equations. We define a scalar variable field, $F(\vec{r},t)$, whose value is unity in the cells fully occupied by the liquid; and is zero when the cell is empty. Cells containing a free surface will have a value of $F$ between zero and unity. Because of the solidification of the molten material, we also need to define a second scalar field, $\Theta(\vec{r},t)$, to describe the solidified region. $\Theta$ is assigned, arbitrarily, equal to unity in a fully liquid cell and is zero in the solidified cells. Any value between zero and unity indicates the presence of a liquid-solid interphase.

The governing equations for mass, momentum, and energy in their time-dependent form are as follows [12]:

*Mass:*

$$\nabla \cdot \Theta \vec{V} = 0 \tag{1}$$

*Momentum:*

$$\frac{\rho}{\Theta}\frac{D\Theta\vec{V}}{Dt} = -\nabla p + \nabla \cdot \mu \nabla \vec{V} + \rho g \tag{2}$$

*VOF:*

$$\frac{\partial F}{\partial t} + \Theta \vec{V} \cdot \nabla F = 0, \tag{3}$$

*Heat transfer and Solidification:* The model uses the *enthalpy transformation model* [22]

$$\rho \frac{Dh}{Dt} = \nabla \cdot \beta \nabla h + \nabla^2 \Phi \tag{4}$$

where h, $\beta$, and $\Phi$ are defined as

$$\begin{cases} \text{solid phase;} \quad h \le 0; & \beta = \dfrac{\kappa_s}{C_s}; \quad \Phi = 0 \\ \text{interphase;} \quad 0 < h < H_f; & \beta = 0; \quad \Phi = 0 \\ \text{liquid phase;} \quad h \ge H_f; & \beta = \dfrac{\kappa_l}{C_l}; \quad \Phi = -\dfrac{H_f \kappa_l}{C_l} \end{cases} \tag{5}$$

All symbols are defined in the nomenclature section. As observed from the definition in Eqn. (5), the last term in Eqn (4) is non-zero only in the intephase zone. Note that within the solidified layer and the substrate, the velocity is zero and the energy equation is reduced to the heat conduction equation.

## Initial and Boundary Conditions

Initial impact velocity, particle diameter and temperature, substrate temperature, and VOF data are prescribed. Substrate temperature far away from the impact area is assumed to be constant, while there is a pressure jump at the free surface described by the Laplace equation [11]. The gas pressure surrounding the droplet is assumed to be uniform.

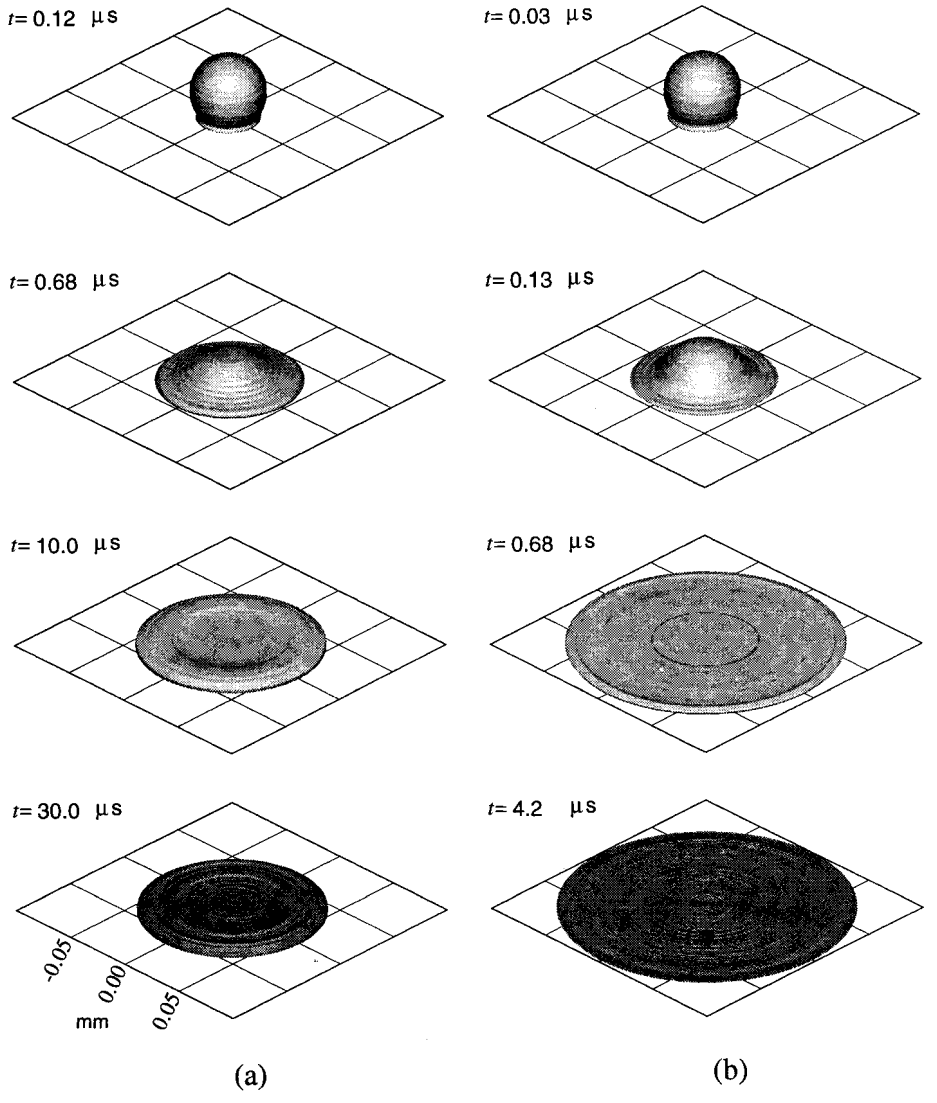


FIGURE 1. Predicted sequence of deformation and solidification for the alumina droplet; 50 μm diameter; 2550°C initial temperature; 90 degrees contact angle; no contact resistance; (a) 50 m/s impact velocity; (b) 200 m/s impact velocity.

An important boundary condition here is the contact angle between the spreading liquid and the substrate. Its magnitude depends on the system under consideration (substrate, droplet, and the surrounding gas). It may also depend on time.

## RESULTS AND DISCUSSION

Figure 2 shows the spreading and solidification of a 50 μm alumina with an initial temperature of 2550 K and an impact velocity of 50 m/s (Fig. 1-a) or 200 m/s (Fig. 1-b). A constant contact angle of 90 degrees was assumed; thermal contact resistance was assigned zero. Initially, the droplet spreads to a maximum splat diameter. Once the inertia of the droplet is diminished, surface tension forces the splat to recoil. Spreading and recoil are basic features of any droplet impact and the extent of maximum spread and recoil depend on the magnitude of *Reynolds (Re)* and *Weber (We)* numbers, respectively. The spreading time is almost inversely proportional to the impact velocity. Hence, the time for spreading of the 200 m/s droplet is 4 times shorter than the 50 m/s case.

Effect of solidification on the spreading was negligible (see Fig. 1); especially at the higher impact speed. An order of magnitude analysis would show [12] that the solidification time is much longer than spreading time if $Ste/Pr << 1$; where *Ste* is the Stefan number and *Pr is Prandtl* number defined in the nomenclature. For the particular cases considered here, this ratio is 0.25. Interestingly, this criteria does not involve the *Reynolds* number.

Capillary effects for the above two cases were found to be negligible. Pasandideh-Fard et. al. [11] have shown that the effect of contact angle on the spreading is unimportant provided that $We >> Re^{0.5}$. For the 200 m/s case (Fig. 1-b), $We=11305$ and $Re=975$; while for the 50 *m/s* case (Fig 1-a) $We=705$, $Re=245$; which satisfy this criterion. In general, the above condition is satisfied for thermal plasma spray process. This is a very important

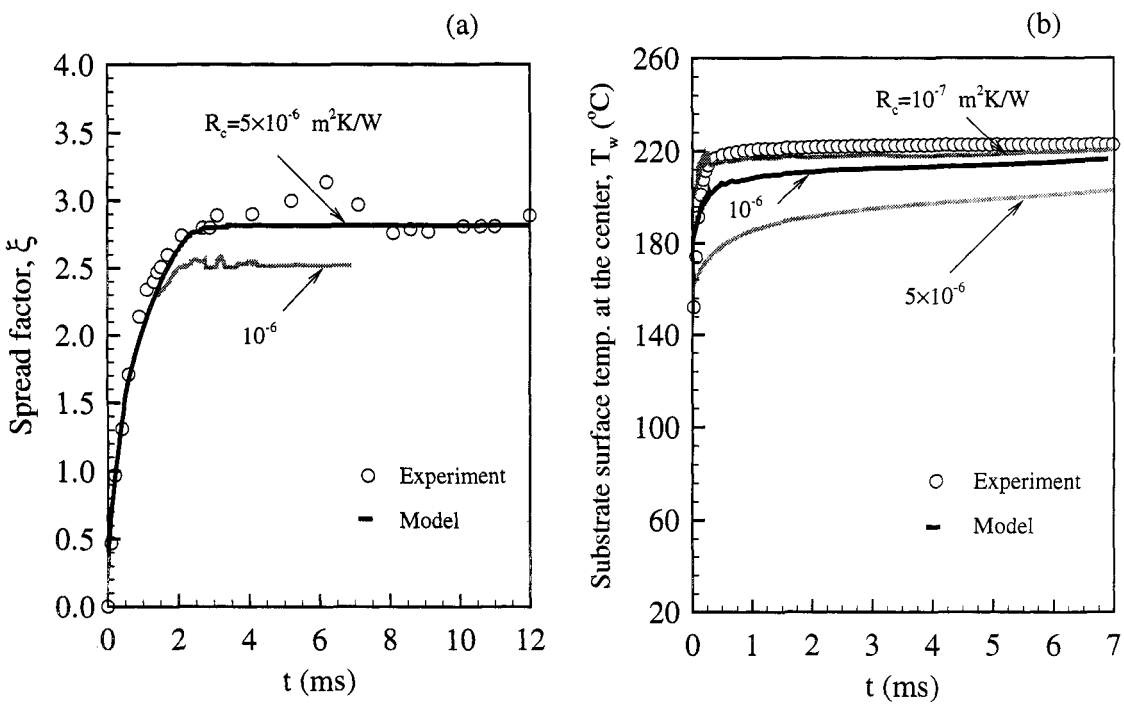


FIGURE 2. Comparison of (a) the predicted spread factor, ξ; and, (b) temperature at the impact point with measurements for a tin droplet; 2.1 mm diameter; 240°C initial temperature; 150°C substrate temperature [12].

result; since it implies that the exact knowledge of contact angle is not necessary in order to make accurate predictions of the splat shapes. Because of the variety in powders and substrate materials used in spraying, information on the contact angles is scarce.

One of the most important factors affecting the solidification is the substrate surface conditions. For better bonding, the substrate is grid blasted before spraying. This leads to the presence of a thermal contact resistance between the splat and the substrate. Its effect is to delay the solidification process. Contact resistance is difficult to measure directly. For any particular case, however, it could be estimated by comparing measured temporal evolution of the spread factor with predictions obtained assuming different contact resistance between the substrate and the splat [10].

Figure 2-a shows the effect of contact resistance on the spread factor for a tin droplet with an initial temperature of 240 C; substrate (stainless steel) temperature of 150 C; and initial diameter of 2.1 mm. The predicted and measured spread factors agree best when the contact resistance is assumed to be $5 \times 10^{-6}$ $m^2K/W$. On the other hand, predicted and measured temperatures at the impact point agree best for a contact resistance of $0.1 \times 10^{-6}$ $m^2K/W$ (Fig. 2-b). The implication of this difference is that the contact resistance is a function of position and it may also change with time. It is also dependent on the substrate temperature [12].

## CONCLUSIONS

A 2-D, axi-symmetric model of droplet impact and solidification was developed. The model assumes laminar, incompressible fluid flow. The solidification is assumed to occur under equilibrium conditions. Typically, droplet spreads to a maximum diameter before recoiling by surface tension. For thermal spray conditions, spreading time is typically a few times smaller than the solidification time and is proportional to the ratio of droplet diameter to the impact speed. Under thermal spray conditions, capillary effects were found to be small. Thus, exact values of the contact angle are not necessary to predict the temporal evolution of the spreading. A comparison between predictions and measurements shows the importance of the thermal contact resistance on solidification. It was found that the thermal contact resistance is a function of position, time, and substrate conditions, e.g., temperature.

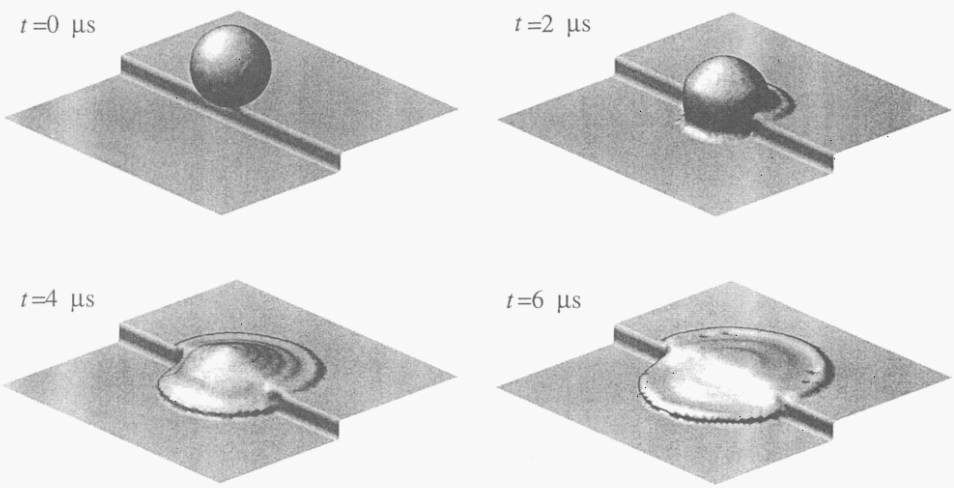


FIGURE 3. 3D impact of an alumina droplet on an edge; droplet diameter 100 μm; impact velocity 20 m/s; edge height 25 μm. Solidification was not considered [19].

To predict the structure of coatings, e.g., porosity, it is necessary to extend the model to 3-D. Such a model would allow predictions of the splat shape on any arbitrary surface. The extension of the model to 3-D has been started and a 3-D fluid dynamic model (without heat transfer) has been accomplished [18, 19]. Figure 3 shows the predictions of this model for an alumina droplet impacting onto an edge. Implementation of a solidification model is currently underway. Future work should also include the study of undercooling effects and non-equilibrium rapid solidification [23].

## ACKNOWLEDGEMENTS

Financial support was provided by the Natural Science and Engineering Research Council of Canada. The 2D simulations were due to M. Pasandideh-Fard (Ph.D. candidate); 3D simulation were due to M. Bussmann (Ph.D. candidate); and, experimental results were due to Professor S. Chandra.

## NOMENCLATURE

C specific heat,
D splat diameter at time t>0,
$\frac{D}{Dt}$ substantial derivative; $(=\frac{\partial}{\partial t}+\vec{V}\cdot\nabla)$,
F Volume of Fluid (VOF),
g acceleration of gravity; (=9.81 $m/s^2$),
$H_f$ heat of fusion,
h enthalpy,
$p$ Pressure
$Pr$ Prandtl number; $(=\frac{\mu C_p}{\kappa})$
$R_c$ Thermal Contact Resistance,
$Re$ Reynolds number; $(=\frac{\rho V_0 D_0}{\mu})$,
$\vec{r}$ position vector,
$Ste$ Stefan number; $(=\frac{C\Delta T}{H_f})$
t time,
$\vec{V}$ velocity vector,
$We$ Webber number; $(=\frac{\rho D_0 V_0^2}{\gamma})$

### Greek Symbols

$\rho$ density,
$\mu$ viscosity,
$\gamma$ surface tension coefficient,
$\Theta$ liquid/solid fraction,
$\kappa$ thermal conductivity
$\zeta$ spread factor; $(=D(t)/D_0)$
$\nabla$ Del operator.

### Subscripts

0 initial value at time zero,
$l$ liquid,
$s$ solid

## REFERENCES

1. C. Moreau, P. Cielo, and M. Lamontagne, *J. Thermal Spray*, **1**, 59 (1992).
2. M. Vardelle, A. Vardelle, A.C. Leger, P. Fauchais, and D. Gobin, *J. Thermal Spray*, **3**, 50 (1994).
3. L. Bianchi, A. Grimaud, F. Blein, P. Lucchese, and P. Fauchais, *J. Thermal Spray*, **4**, 50 (1995).
4. Y.C. Lee and E. Pfender, *Plasma Chem Plasma Proc*, **5**, 211 (1985).
5. H. Jones, *J. Phys. D: Appl. Phys.*, **4**, 1657 (1971).
6. J. Madjeski, *Int. J. Heat/Mass Transfer*, **19**, 1009 (1976).
7. S. Chandra and C.T. Avedisian, *Proc. R. Soc. London A* **432**, 13 (1991).
8. T. Yoshida, T. Okada, H. Hatamani, and H. Kumaoka, *Plasma Sources: Sci. & Tec.*, **1**, 195 (1992).
9. H. Fukanuma, *Proc. Int. Thermal Spray Conf.*, Florida, USA, 767, (1992).
10. M. Pasandideh-Fard and J. Mostaghimi, *Plasma Chem. Plasma Proc.*, **16**, 83S (1996).

11. M. Pasandideh-Fard, M. Qiao, S. Chandra, and J. Mostaghimi, *Phys. Fluids* **8**, 650 (1996).
12. M. Pasandideh-Fard, R. Bhola, S. Chandra, and J. Mostaghimi, *Proc. ASME National Heat Transfer Conf.*, **HTD-Vol. 347**, 20 (1997).
13. F.H. Harlow and J.P. Shanon, *J. Appl. Phys.*, **38**, 3855 (1967).
14. G. Trapaga and J. Szekely, *Metallurgical Trans. B* **22**, 901 (1991).
15. H. Liu, E.J. Lavernia, R.H. Rangel, E. Muehlberger, and A. Sickinger, *Proc. National Thermal Spray Conf.*, California, USA, 457 (1993).
16. J. Fukai, Z. Zhao, D. Poulikakos, C.M. Megaridis, and O. Miyatake, *Phy. Fluids*,A **5**, 2588 (1993).
17. J. Fukai, Y. Shiiba, T. Yamamoto, O. Miyatake, D. Poulikakos, C..M. Megaridis, and Z. Zhao, *Phy. Fluids*,A **7**, 236 (1996).
18. M. Bussmann, S. Chandra, and J. Mostaghimi, *Proc. ASME Fluids Engng.*, Vancouver, BC, **FEDSM97-3073** (1997).
19. M. Bussmann, S. Chandra, and J. Mostaghimi, *Proc. Asea-Pcific Conf. Plasma Sci & Tech*, Tokyo, Japan (1996).
20. D.B. Koethe, R.C. Mjolsness, and M.D. Torrey, *Los Alamos Scientific Laboratory*, **LA-12007-MS, UC-000** (1991).
21. B.D. Nichols, C.W. Hirt, and R.S. Hotchkiss, *Los Alamos Scientific Laboratory*, **LA-8355, UC-32** (1980).
22. F. Chabchoub, S.A. Argyropoulos, and J. Mostaghimi, *Canadian Metalurgica Quarterly*, **33**, 73 (1994).
23. Robert, A. Vardelle, G.X. Wang, S. Sampath, Proc. *National Thermal Spray Conf.*, Indianapolis, USA (1997).